



## OPEN

## SUBJECT AREAS:

MICROGLIA

EXCITABILITY

NEUROPHYSIOLOGY

SPINE STRUCTURE

# The intrinsic microglial molecular clock controls synaptic strength via the circadian expression of cathepsin S

Yoshinori Hayashi<sup>1</sup>, Satoru Koyanagi<sup>2</sup>, Naoki Kusunose<sup>2</sup>, Ryo Okada<sup>1</sup>, Zhou Wu<sup>1</sup>, Hidetoshi Tozaki-Saitoh<sup>3</sup>, Kiyoharu Ukai<sup>4</sup>, Shinichi Kohsaka<sup>5</sup>, Kazuhide Inoue<sup>3,6</sup>, Shigehiro Ohdo<sup>2</sup> & Hiroshi Nakanishi<sup>1,6</sup>

Received

24 June 2013

Accepted

4 September 2013

Published

25 September 2013

Correspondence and requests for materials should be addressed to H.N. (nakan@dent.kyushu-u.ac.jp)

<sup>1</sup>Department of Aging Science and Pharmacology, Faculty of Dental Sciences, Kyushu University, Fukuoka, 812-8582, Japan, <sup>2</sup>Pharmaceutics, Faculty of Pharmaceutical Sciences, Kyushu University, Fukuoka, 812-8582, Japan, <sup>3</sup>Department of Molecular and System Pharmacology, Graduate School of Pharmaceutical Sciences, Kyushu University, Fukuoka 812-8582, Japan, <sup>4</sup>Central Research Institute, Kaken Pharmaceutical Co. Ltd, Kyoto, Japan, <sup>5</sup>Department of Neurochemistry, National Institute of Neuroscience, Kodaira, Tokyo 187-8502, Japan, <sup>6</sup>Japan Science and Technology Agency, CREST, 5, Sanbancho, Chiyoda-ku, Tokyo, 102-0075, Japan.

**Microglia are thought to play important roles in the maintenance of neuronal circuitry and the regulation of behavior. We found that the cortical microglia contain an intrinsic molecular clock and exhibit a circadian expression of cathepsin S (CatS), a microglia-specific lysosomal cysteine protease in the brain. The genetic deletion of CatS causes mice to exhibit hyperlocomotor activity and removes diurnal variations in the synaptic activity and spine density of the cortical neurons, which are significantly higher during the dark (waking) phase than the light (sleeping) phase. Furthermore, incubation with recombinant CatS significantly reduced the synaptic activity of the cortical neurons. These results suggest that CatS secreted by microglia during the dark-phase decreases the spine density of the cortical neurons by modifying the perisynaptic environment, leading to downscaling of the synaptic strength during the subsequent light-phase. Disruption of CatS therefore induces hyperlocomotor activity due to failure to downscale the synaptic strength.**

There is accumulating evidence that microglia do not rest even in the healthy brain<sup>1</sup> and continuously search the synaptic microenvironment using their fine processes<sup>2–4</sup>. Microglia engulf synapses<sup>5</sup> and prune connections between neurons<sup>6</sup> to establish mature patterns of connectivity during postnatal development. Deficiencies of microglia-specific molecules, including Cx3cr1 and KARAP/DAP12, significantly change the synaptic strength in the hippocampus and cerebral cortex<sup>6–8</sup>. Furthermore, disruption of genes specific or related to microglia, including the Hoxb8 gene and the gene encoding the methyl CpG binding protein 2 (MeCP2), results in higher brain dysfunction<sup>9,10</sup>. These observations indicate that a proper microglial function is required for an appropriate brain function and that the constitutive activity of microglia is important for the maintenance of the neuronal circuitry and the regulation of behavior.

Cathepsin S (CatS; EC 3.4.22.27) is a member of the lysosomal cysteine protease family, which is preferentially expressed in cells of mononuclear phagocytic origin. In the central nervous system, CatS is exclusively expressed in microglia. CatS retains its proteolytic activity even after prolonged exposure to a neutral pH. CatS has been reported to degrade several extracellular matrix (ECM) molecules, including fibrillar collagen, elastin, laminin, fibronectin and heparan sulfate proteoglycans, at a neutral pH<sup>11</sup>. CatS-deficient (CatS<sup>-/-</sup>) monocytic cells exhibit impaired subendothelial basement membrane transmigration<sup>12</sup>. Furthermore, CatS plays a pivotal role in the functions of antigen-presenting cells, including dendritic cells and microglia<sup>13,14</sup>. More recently, the secretion of CatS by the spinal microglia has been shown to be involved in the maintenance of neuropathic pain<sup>15</sup>. However, little is known about the role of CatS in the normal brain function.

We herein provide the first evidence that the cortical microglia contain an intrinsic molecular clock and exhibit the circadian expression of CatS. The circadian expression of CatS induces diurnal variations in the synaptic strength of the cortical neurons via the proteolytic modification of the perineuronal environment. Disruption of CatS therefore induces hyperlocomotor activity due to failure to downscale the synaptic strength during sleep.

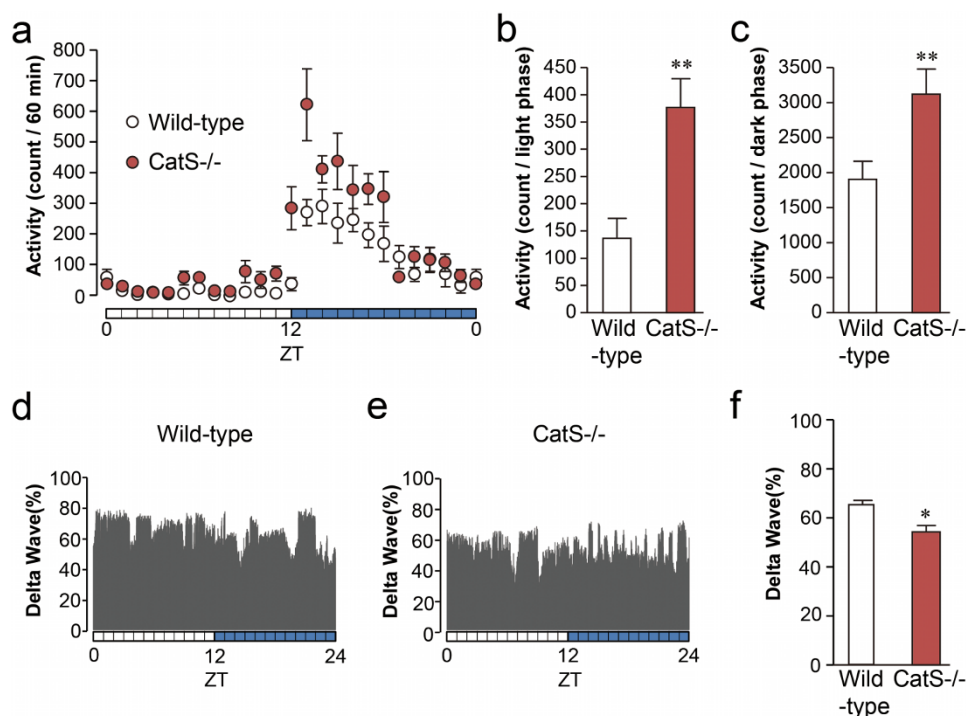


**Figure 1 | Increase in locomotor activity and reduction of sleep intensity in *CatS*<sup>-/-</sup> mice.** (a–c) *CatS*<sup>-/-</sup> mice exhibited elevated spontaneous locomotor activity both during the light-phase (b) and the dark-phase (c). The asterisks indicate statistically significant differences from wild-type (\*\*,  $P < 0.01$ ; unpaired *t*-test). The data are presented as the mean  $\pm$  S.E.M. (wild-type  $N = 8$  animals, *CatS*<sup>-/-</sup>  $N = 8$  animals). (d, e) the EEG delta power from freely moving wild-type (d) and *CatS*<sup>-/-</sup> (e) mice. The graph was plotted in 1 min intervals. (f) The mean relative EEG delta power in the light phase (ZT2–4) in wild-type and *CatS*<sup>-/-</sup> mice. The asterisks indicate statistically significant differences between values (\*,  $P < 0.05$ ; unpaired *t*-test). The data are the means  $\pm$  S.E.M. (wild-type  $N = 6$  animals, *CatS*<sup>-/-</sup>  $N = 5$  animals).

## Results

### Increased spontaneous locomotor activity and reduced sleep in *CatS*<sup>-/-</sup> mice.

In the course of experiments to evaluate the possible role of *CatS* in the regulation of behavior, we found that *CatS*<sup>-/-</sup> mice exhibit hyperlocomotor activity. In this study, both wild-type and *CatS*<sup>-/-</sup> mice displayed increased spontaneous locomotor activity, including surges of spontaneous locomotor activity, when the lights were turned off (Fig. 1a). The mean total spontaneous locomotor activity of *CatS*<sup>-/-</sup> mice was significantly larger than that of wild-type mice during both the light and dark phases (Fig. 1b, c).

Accumulating evidence showing that the sleep-wake cycle regulates the synaptic strength, including neuronal transmission<sup>16,17</sup> and spine density<sup>18,19</sup>, prompted us to further investigate the role of *CatS* in the sleep-wake cycle using electroencephalogram (EEG) spectral analyses. The EEG delta power, which is characterized by EEG with a frequency range of 0.1–4 Hz, was recorded from the cerebral cortex of freely moving wild-type and *CatS*<sup>-/-</sup> mice for 24 h. In wild-type mice, the mean relative EEG delta power was significantly higher during the light phase than during the dark phase (Fig. 1d, light:  $62.6 \pm 3.8\%$ , dark:  $57.8 \pm 2.7\%$ ,  $P < 0.05$ , unpaired *t*-test). In contrast, the mean relative EEG delta power showed no significant difference in both phases in *CatS*<sup>-/-</sup> mice (Fig. 1e, light:  $54.4 \pm 2.5\%$ , dark:  $51.9 \pm 4.3\%$ ). It was also noted that the mean relative EEG delta power during the light phase (ZT2–4) was significantly lower in *CatS*<sup>-/-</sup> mice than in wild-type mice (Fig. 1f). These observations indicate that the EEG delta power, a marker of sleep intensity, is significantly decreased during the light (sleeping) phase in *CatS*<sup>-/-</sup> mice compared with wild-type mice. Therefore, it is considered that the reduced EEG delta power is responsible for the increased spontaneous locomotor activity observed in *CatS*<sup>-/-</sup> mice.

**Disappearance of diurnal variations of the synaptic strength in *CatS*<sup>-/-</sup> mice.** We further examined the effects of genetic depletion of

*CatS* on the synaptic activity of the cortical neurons by the patch clamp recordings. In wild-type mice, the mean frequency and amplitude of miniature excitatory postsynaptic currents (mEPSCs) recorded from the cortical neurons were significantly larger at ZT14 than at ZT2 under the light-dark (LD) conditions (Fig. 2a, b, e, f). In contrast, no significant differences were observed in the *clock*-mutant mice (Supplementary Fig. S1a–d), which exhibited an abnormal circadian gene expression<sup>20</sup>. Diurnal variation in the mean frequency and amplitude of mEPSCs was also observed under the constant darkness (DD) conditions (Supplementary Fig. S1e, f). These observations suggest that the diurnal alteration of synaptic strength is regulated by the circadian clock system. In wild-type mice, the mean spine density of the cortical neurons was also significantly larger at ZT14 than at ZT2 (Fig. 2g, h, k). In *CatS*<sup>-/-</sup> mice, however, there were no significant differences in either the mean frequency or mean amplitude of mEPSCs at ZT2 and ZT14 (Fig. 2c–f). The mean amplitude of mEPSCs in *CatS*<sup>-/-</sup> mice at ZT2 was significantly larger than that observed in wild-type mice. Furthermore, there were no significant differences in the mean spine density of the cortical neurons in *CatS*<sup>-/-</sup> mice at ZT2 and ZT14 (Fig. 2i, j, k). The mean spine density at ZT2 was significantly larger in *CatS*<sup>-/-</sup> mice than wild-type mice (Fig. 2k). Microglia play a role in the proteolytic modification of ECM molecules by secreting various extracellular proteases to influence the neuronal plasticity and synaptic properties of neurons<sup>21–23</sup>. *CatS*-dependent circadian changes in the synaptic strength of the cortical neurons suggest the existence of an intrinsic microglial molecular clock that regulates the expression of *CatS*.

**Existence of an intrinsic molecular clock in microglia.** To evaluate the possible existence of an intrinsic molecular clock in microglia, we subjected microglia isolated from the adult murine cerebral cortex according to the magnetic cell sorting (MACS) method using

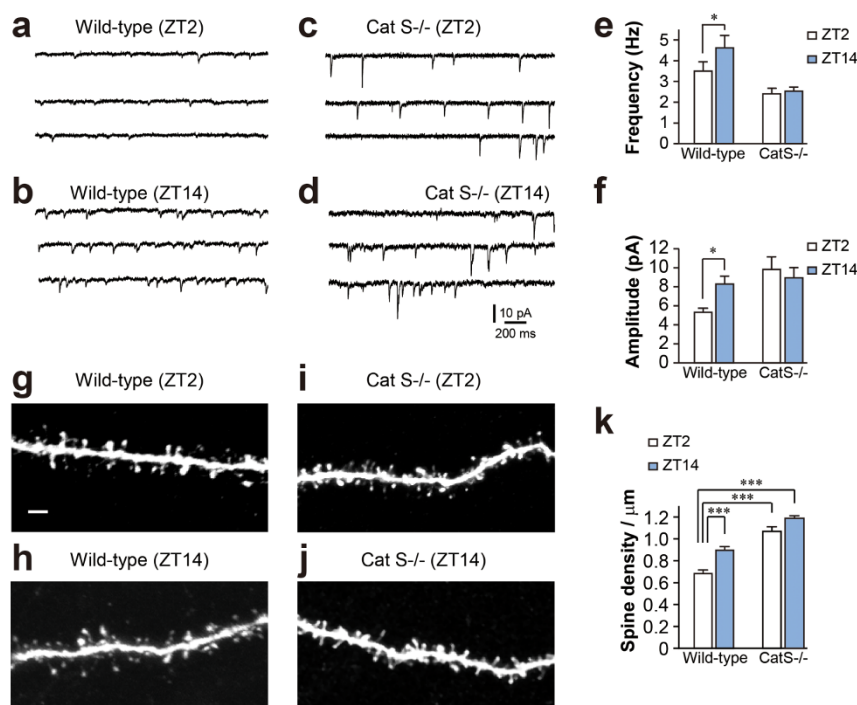


**Figure 2** | CatS-dependent diurnal alterations in the synaptic activity and spine density of the cortical neurons. (a–d) Typical traces of mEPSCs recorded from the cortical neurons obtained from wild-type (a), (b) and CatS<sup>-/-</sup> mice (c), (d) at ZT2 and ZT14. (e), (f) The mean frequency (e) and amplitude (f) of mEPSCs obtained from the cortical neurons. The data are presented as the mean  $\pm$  S.E.M. (N = 4 animals, n = 10–18 neurons each; \*,  $P < 0.05$ ; \*\*,  $P < 0.01$ ; two-way ANOVA). (g–j) CLSM images of dendrites were captured from lucifer yellow-injected neurons obtained from wild-type (g), (h) and CatS<sup>-/-</sup> mice (i), (j) at ZT2 and ZT14. Scale bar = 2  $\mu\text{m}$ . (k) The mean spine density of the cortical neurons in wild-type and CatS<sup>-/-</sup> mice at ZT2 and ZT14. Wild-type (ZT2) n = 44 dendrites in 20 neurons, 1,840 spines, wild-type (ZT14) n = 54 dendrites in 18 neurons, 2,512 spines, CatS<sup>-/-</sup> (ZT2) n = 109 dendrites in 21 neurons, 8,966 spines, CatS<sup>-/-</sup> (ZT14) n = 116 dendrites in 23 neurons, 9,937 spines. The asterisks indicate statistically significant differences between values (\*\*\*,  $P < 0.001$ ; two-way ANOVA).

magnetically labeled with CD11b microbeads in order to measure the expression of clock genes. The isolated cortical microglia exhibited a rhythmic expression of *Period1* (*Per1*), *Per2*, and *Rev-erba*, target genes of CLOCK/BMAL1 heterodimers, with circadian oscillation that peaked at ZT14 for *Per1* and *Per2* and ZT18 for *Rev-erba* (Fig. 3). The expression of *Bmal1*, a core transcription factor of the molecular clock that is negatively controlled by a *Per* or *Cryptochrome* (*Cry*)-dependent feedback loop<sup>24,25</sup>, was induced opposite to *Per*. The same diurnal variation of clock genes was also observed in microglia isolated from the adult mice housed under DD conditions (Fig. 3). In contrast, microglia isolated from *clock*-mutant mice showed no significant time-of-day differences (Fig. 3). These observations indicate that the cortical microglia have an intrinsic molecular clock regulated by CLOCK/BMAL1-driven transcriptional negative feedback loops.

**Circadian expression of microglial CatS.** We next analyzed whether the expression of CatS is regulated by the intrinsic microglial molecular clock. As shown in Figure 4, the cortical microglia were found to exhibit a circadian oscillation of CatS transcripts with a peak at ZT14 (Fig. 4a) under both LD (Fig. 4b) and DD (Fig. 4c) conditions that was well synchronized with *Per1* and *Per2* (Fig. 2). In contrast, no diurnal variation of the *CatS* gene expression was observed in the cortical microglia isolated from the *clock*-mutant mice (Fig. 4b, c). On the other hand, tissue-plasminogen activator (tPA), plasminogen activator inhibitor-1 (PAI-1) and matrix metalloproteinase-9 (MMP-9), ubiquitously expressed proteases, did not synchronize with the *Per1* and *Per2* oscillation in microglia (Supplementary Fig. S2). To further analyze the relationship between the clock genes and *CatS*, a luciferase reporter assay system was constructed (Fig. 4d). The transcriptional activity of *CatS-Luc* that contained the E-box was

significantly enhanced by CLOCK/BMAL1 proteins, but not by CLOCK $\Delta$ 19/BMAL1 (Fig. 4e). In addition, the CLOCK/BMAL1-mediated transactivation of the *CatS-Luc* was significantly repressed by the addition of RER2 and CRY1 (Fig. 4e). These observations indicate that the diurnal alteration in the *CatS* gene expression is regulated by the intrinsic microglial molecular clock, consisting of transcriptional negative feedback loops with the CLOCK/BMAL1 complex binding to E-boxes in its promoter region.

#### Possible involvement of CatS in diurnal variations of the synaptic strength through the proteolytic modification of perisynaptic environment.

Microglia are well known to possess highly motile processes<sup>2,3</sup> that survey the synapse microenvironment<sup>4</sup>, however, there is no free space around the synapse. Therefore, the CatS-mediated degradation and modification of ECM molecules is necessary for microglial process extension. To examine this issue, the effects of Z-FL-COCHO, a specific inhibitor of CatS, on the ATP-induced microglial process extension were assessed using a two-photon *in vivo* imaging system. The ATP-induced microglial process extension was significantly suppressed by AR-C 66096, a specific inhibitor of P2Y<sub>12</sub>R (Supplementary Fig. S3a), as previously reported<sup>26</sup>. Z-FL-COCHO, a specific inhibitor of CatS, was found to significantly inhibit the ATP-induced microglial process extension during the dark phase (Supplementary Fig. S3b), and only partially during the light phase. These observations suggest that the secretion of CatS from microglia induces the proteolytic modification and degradation of ECM molecules during the dark phase.

To further examine whether CatS secreted from microglia modulates the synaptic activity via extracellular proteolysis, the effects of human recombinant CatS (hrCatS) on mEPSCs recorded from the cortical neurons were examined. No significant changes in mEPSCs

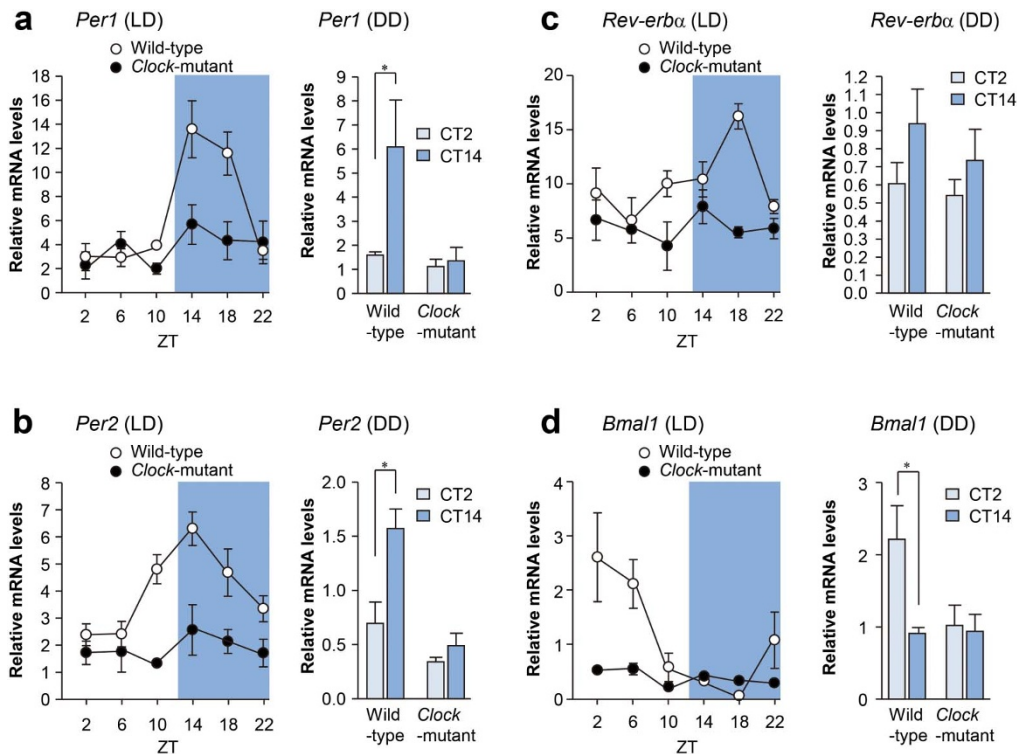


**Figure 3 | Circadian oscillation of the expression of clock genes in the cortical microglia.** (a–d) Circadian oscillation of the mRNA levels of the four core clock genes, *Period1* (*Per1*) (a), *Period2* (*Per2*) (b), *Rev-erbα* (c) and *Bmal1* (d) in microglia isolated from the cerebral cortex of the adult mice housed under LD or DD conditions. Microglia were obtained from wild-type and the *clock*-mutant mice at every 4 h using MACS. Open circles: wild-type, Filled circles: *clock*-mutant mice. The relative mean mRNA levels were normalized to the  $\beta$ -actin level. The data are presented as the mean  $\pm$  S.E.M. ( $n = 3$  independent experiments each,  $P = 0.00021$  (a), 0.00042 (b), 0.019 (c), and 0.009 (d) under LD conditions, two-way ANOVA,  $n = 3$  independent experiments each, \*,  $P < 0.05$ ; \*\*,  $P < 0.01$  under DD conditions; two-way ANOVA).

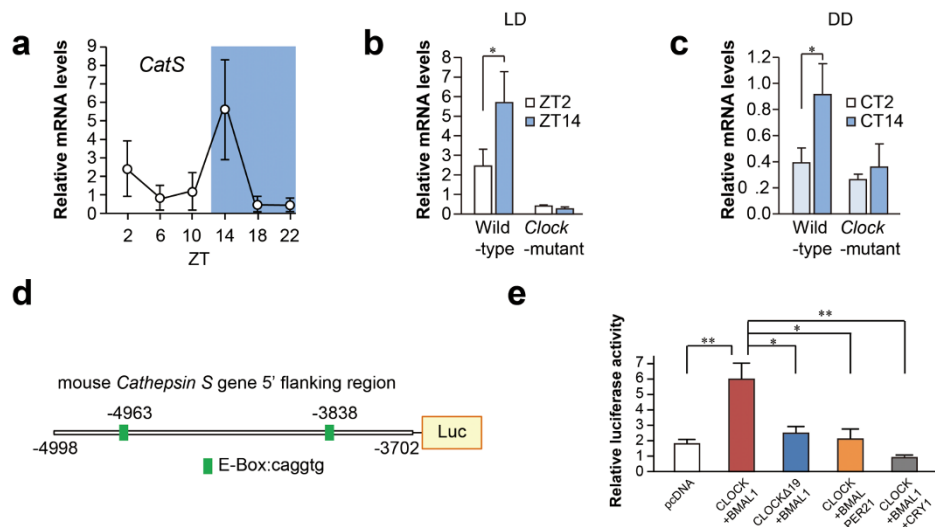


**Figure 4 | Possible associations with the circadian variation of the microglial *CatS* expression.** (a) Circadian oscillation of the expression of *CatS* in the cortical microglia in the mice housed under LD conditions. The data are presented as the mean  $\pm$  S.E.M. ( $n = 3$  independent experiments each:  $P = 0.0041$ ; two-way ANOVA). (b), (c) The relative mean mRNA levels of *CatS* in microglia isolated from wild-type and the *clock*-mutant mice brains at ZT2 and ZT14 (b) or CT2 and CT14 (c) from the mice housed under LD or DD conditions. The data are presented as the mean  $\pm$  S.E.M. ( $n = 3$  independent experiments each: \*,  $P < 0.05$ ; two-way ANOVA). (d) The promoter region of the *CatS* gene was fused to a luciferase reporter gene (*CatS-Luc*) and transfected into NIH3T3 cells. (e) *CatS-Luc* was activated by CLOCK/BMAL1, but not CLOCK $\Delta$ 19/BMAL1 proteins. The CLOCK/BMAL1-mediated transactivation was repressed by CRY1. The data are presented as the mean  $\pm$  S.E.M. ( $n = 3$  independent experiments each: \*,  $P < 0.05$ ; one-way ANOVA).

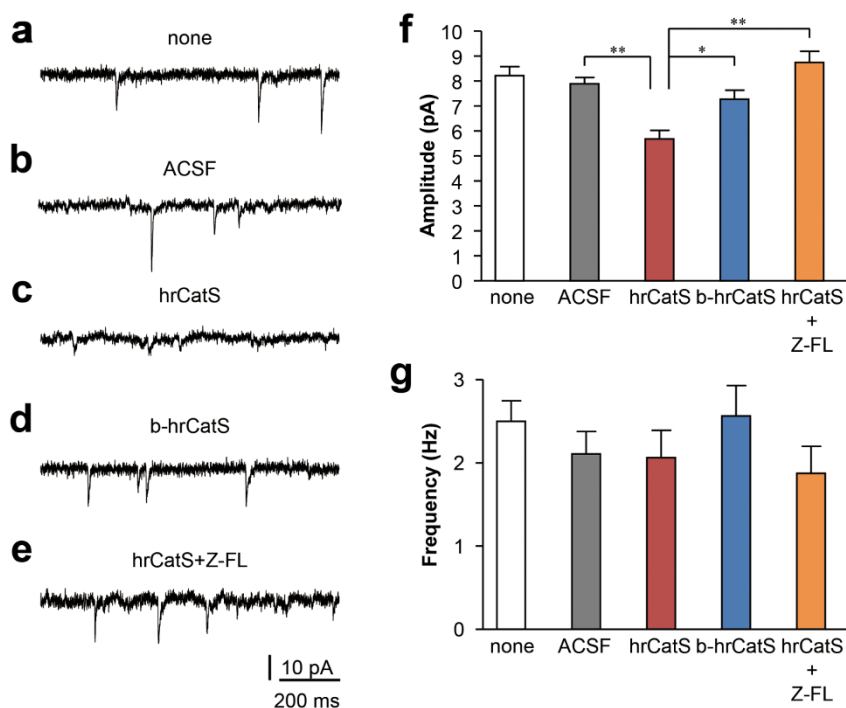


**Figure 5 | Inhibitory effect of hrCatS on the synaptic activity of the cortical neurons.** (a–e) Typical traces of mEPSCs recorded from the cortical neurons of the non-treated controls (a), after incubation with ACSF (b), 50 nM hrCatS (c), heat-denatured (boiled) hrCatS (b-hrCatS) (d) or 50 nM hrCatS in combination with 20  $\mu$ M Z-FL-COCHO (Z-FL) (e) for 3 h. (f), (g) The mean amplitude (f) and frequency (g) of mEPSCs obtained from the cortical neurons of the non-treated controls, incubation with ACSF, 50 nM hrCatS, heat-denatured (boiled) hrCatS (b-hrCatS) or 50 nM hrCatS in combination with 20  $\mu$ M Z-FL-COCHO (Z-FL) for 3 h. The data are presented as the mean  $\pm$  S.E.M. (N = 3–6 animals, n = 69 neurons for non-treated controls, n = 13–18 neurons each for the other conditions; \*,  $P < 0.05$ ; \*\*,  $P < 0.01$ ; one-way ANOVA).

were observed following incubation with the artificial cerebrospinal fluid (ACSF) for 3 h (Fig. 5b, f, g). The mean amplitude of mEPSCs recorded from the cortical neurons was significantly inhibited by the incubation of acute cortical slices with 50 nM hrCatS for 3 h (Fig. 5c, f), but not with heat-denatured (boiled) hrCatS (Fig. 5d, f). Furthermore, the inhibitory effects of hrCatS on the mean amplitude of mEPSCs recorded from the cortical neurons were completely recovered by the addition of 20  $\mu$ M Z-FL-COCHO, a specific inhibitor of CatS (Fig. 5e, f). On the other hand, the mean frequency of mEPSCs recorded from the cortical neurons was not significantly affected by hrCatS (Fig. 5c, g).

## Discussion

Our observations herein demonstrated that an intrinsic microglial molecular clock drives the circadian expression of CatS, resulting in the downscaling of the synaptic strength of the cortical neurons via the proteolytic modification of the perisynaptic environment. The downscaling of dendritic spine structures induces a decrease in the synaptic strength of the cortical neurons during the light phase, which is necessary for the active synaptic functions observed during the subsequent dark phase.

CatS<sup>-/-</sup> mice exhibited elevated spontaneous locomotor activity compared with wild-type mice. Furthermore, the present EEG power spectral analyses revealed that the mean relative EEG delta power recorded during the light phase was significantly lower in CatS<sup>-/-</sup> mice than in wild-type mice. This indicates that CatS<sup>-/-</sup> mice retain higher waking intensity, because the EEG delta power is considered to be a marker of sleep intensity. Similar increased spontaneous locomotor activity and reduced sleep level are also observed in the clock-mutant mice<sup>27,28</sup>. In the present study, the mean amplitude of mEPSCs recorded from the cortical neurons during the light phase was also significantly higher in CatS<sup>-/-</sup> mice than in wild-type mice.

These observations are consistent with the notion that waking increases the mean amplitude of mEPSCs<sup>16</sup> and its related molecules<sup>17</sup>. Moreover, Liu et al. reported that sleep deprivation enhances synaptic activity<sup>16</sup>. On the other hand, sleep plays an important role in downscaling the synaptic strength and number of synaptic connections in the brain<sup>16,17</sup>. Furthermore, the sleep disturbance and resultant lack of downscaling of synaptic strength in CatS<sup>-/-</sup> mice are attributable to the increased spontaneous locomotor activity in CatS<sup>-/-</sup> mice.

During postnatal development, microglia engulf spines in a neuronal activity-dependent manner and eliminate them<sup>5</sup>. In the present study, however, we were unable to obtain any direct evidence supporting the phagocytic elimination of synaptic elements by microglia in the cerebral cortex of adult mice. It is known that tPA, MMP-9 and CatS are involved in the proteolytic modification of extracellular matrix proteins, which influences the neuronal plasticity and synaptic properties of neurons<sup>22,29</sup>. However, neither tPA nor MMP-9 synchronized with the circadian oscillation of *Per*, because they are ubiquitously expressed in the brain. CatS is specifically expressed in microglia among brain cells<sup>11,30</sup>, which are synchronized with the oscillation pattern of *Per*. We previously reported that microglia fail to spread on injured motoneurons and retain with relatively large cell bodies in CatS<sup>-/-</sup> mice following nerve transection. Insufficient degradation of tenascin-R, an antiadhesive perineuronal net for microglia, is considered to prevent microglia from spreading on the surface of injured motoneurons in CatS<sup>-/-</sup> mice. Therefore, CatS is able to degrade ECM molecules that influence the migratory and adhesion properties of microglia, even at a neutral pH<sup>31</sup>. Extracellular CatS is able to degrade proteoglycan<sup>11,30,31</sup>, a key component of the perisynaptic extracellular matrix. Spine motility is regulated by ECM molecules<sup>32,33</sup>. Heparan sulfate proteoglycan, particularly in syndecan-2, is involved in spine formation<sup>34,35</sup>.



Furthermore, conditional *Ext1*, an enzyme essential for heparan sulfate synthesis, mutant mice exhibited reductions in the number of AMPA receptors and abnormal behavior<sup>36</sup>. Functional changes in the glutamate receptor<sup>16,17</sup> and spine density<sup>18,19</sup> during sleep-wakefulness may be attributed to the regulation of ECM molecules by CatS secreted from microglia. Our study showed that the incubation of cortical slices with hrCatS significantly reduces the mean amplitude of mEPSCs recorded from the cortical neurons. The inhibitory effects of hrCatS were completely recovered by the addition of Z-FL-COCHO, a specific inhibitor of CatS. These observations suggest that CatS reduces the mean amplitude of mEPSCs recorded from the cortical neurons via the proteolytic modification of perisynaptic ECM molecules.

In conclusion, the intrinsic microglial molecular clock-driven circadian expression of CatS induces diurnal variations in synaptic strength via the proteolytic modification of the perisynaptic environment. The CatS-mediated modification of the perisynaptic environment induces the downscaling of synaptic strength during sleep, which is necessary for the acquisition of subsequent novel information after waking. Therefore, our observations implicate microglia as a major circuit breaker in the brain. Further research on this topic will aid in understanding neuropsychiatric disorders based on sleep disturbance.

## Methods

**Animals.** All efforts were made to minimize animal suffering and to reduce the number of animals used. Male *Clock*-mutant mice<sup>20</sup> bred on an ICR background from Jackson Laboratory, *CatS*<sup>-/-</sup> mice<sup>31</sup> on a DBA background, and *Iba1*-EGFP transgenic mice<sup>38</sup> were used. The mice were housed under either normal LD conditions (lights on at 07:00 and lights off at 19:00) or DD conditions in a temperature-controlled room (24 ± 1°C) with a humidity of 60 ± 10% and provided food and water *ad libitum*. The mice were adapted to LD conditions for two weeks before the experiments. Under LD conditions, the ZT0 (Zeitgeber time) was designated as lights on and ZT12 was designated as lights off. For the mice housed under DD conditions, the circadian time (CT) was used instead of ZT, and CT0 was characterized as the beginning of the subjective light phase, while CT12 was defined as the beginning of the subjective dark phase. All animals were treated in accordance with the guidelines issued by the animal care and use committee of Kyushu University.

**Locomotor activity.** The spontaneous locomotor activity was measured during a 60-min period for 24 h using an Animex apparatus (Animex Auto MK-110, Muromachi Kikai, Tokyo, Japan) under the cage. The mice were kept in their home cage with food and water.

**EEG power spectral analysis.** The mice (8–10 weeks old) were anesthetized with sodium pentobarbital (50 mg/kg, i.p.). Two stainless steel miniature screws (diameter 1 mm) placed over the right frontal cortex and the right parietal cortex (1.5 mm lateral to the midline and 1 mm anterior from bregma or lambda) served as epidural EEG electrodes. Two vinyl-coated braided stainless steel wire electrodes (Cooner Wire) were placed in the nuchal muscle for electromyogram (EMG) recording. All electrodes were attached to a microconnector and fixed to the skull with dental cement. EEG and EMG recordings were performed 1 week after implantation. The EEG and EMG data were amplified, filtered (0.1–50 Hz) and stored on a computer (sampling rate: 1024/s) from freely moving mice for 24 h using the DasyLab10 device (Dasytec). The traces of EEG along with their spectra and the power within the delta range (0.1–4 Hz) was continuously monitored during the experiment. EEG power spectra were then calculated (FFT routine, Hanning window of 4 s epoch).

**Isolation of microglia from adult animals.** The mice (8–10 weeks old) mice were anesthetized and perfused transcardially with phosphate-buffered saline (PBS), then the mice were decapitated ( $n = 3$  at each time point). Microglia were isolated according to the MACS method using magnetically labeled with CD11b microbeads. The isolated cells were incubated with anti-mouse CD45-fluorescein (FITC) and anti-mouse CD11b-phycoerythrin (PE) at optimal dilutions. The purity of microglia was calculated to be 78.24% (Supplementary Fig S4a) using fluorescent activated cell sorting (FACS) (Becton-Dickinson). The mean mRNA expression level of *c-fos*, a marker of cellular activation, was significantly higher in the cells isolated for 6 h than those isolated for 3 h (Supplementary Fig S4b). Therefore, all manipulations were terminated within 3 h in the present study.

**Quantitative RT-PCR analysis.** Total RNA was extracted from microglia using RNAsiso (Takara Bio Inc., Shiga, Japan). Complementary DNA (cDNA) was prepared via reverse transcription of the total RNA using a ReverTra Ace<sup>®</sup> qPCR RT kit (Toyobo Co. Ltd., Osaka, Japan). The diluted cDNA samples were analyzed by real-time RT-PCR. Real-time PCR was performed using the THUNDERBIRD<sup>™</sup> SYBR<sup>®</sup> qPCR Mix (Toyobo) and the 7500 Real-time PCR system (Applied Biosystems, Foster

City, CA). To determine the copy numbers, we performed the 2<sup>-ΔΔC<sub>t</sub></sup> method using a calibrator, as previously described<sup>39</sup>. The primer sequences used for the quantitative PCR of the target genes and their amplicons are listed in Supplementary Table S1. The primers were designed to flank a region that contains at least one intron.

**Construction of reporter and expression vectors.** To construct the luciferase reporter vector for the *CatS* gene (*CatS-Luc*), a 5'-upstream fragment of the promoter region of the mouse *CatS* gene spanning bp -4998 to -3702 (Genbank Accession# NM\_021281) was amplified via PCR, and the product was fused to the pGL4.12 vector (Promega). The expression plasmids for *clock* and the clock-related genes were prepared as follows: the coding regions of *clock* and the clock-related genes were obtained via RT-PCR and used after their sequences were confirmed, as previously reported<sup>37</sup>. All coding regions were ligated into the pcDNA3.1 vector (Invitrogen).

**Luciferase reporter assay.** NIH3T3 cells were maintained in DMEM supplemented with 5% FBS at 37°C in a humidified 5% CO<sub>2</sub> atmosphere<sup>38</sup>. NIH3T3 cells do not normally express the *CatS* gene (data not shown). The cells were seeded ( $1 \times 10^5$  cells well<sup>-1</sup>) into 24-well plates then transfected with 100 ng of the reporter construct and 0.5 μg (total) of the expression constructs using the Lipofectamine-LXT reagent (Invitrogen, Carlsbad, CA, USA). The pGL4.74 [hRluc/TK] vector (0.5 ng, Promega) was co-transfected into each well, as an internal control. The total amount of DNA per well was adjusted by adding pcDNA3.1 vector (Invitrogen). The ratio of firefly (expressed by the reporter construct) to *Renilla* expressed by the pGL4.74 [hRluc TK<sup>-1</sup>] luciferase activity in each sample served as a measure of the normalized luciferase activity<sup>37</sup>.

**Intracellular labeling of the cortical neurons.** Cortical segments perfused with 4% PFA were sectioned into 100-μm-thick samples using a vibratome ( $n = 24$ –26 slices from three animals). The cell bodies were visualized with YOYO-1 (1 : 10,000, Molecular Probes) for 3 min then 4% lucifer yellow was injected into the cortical neurons through a glass pipette similar to the method previously described<sup>39</sup>. The sections were incubated with 4% PFA for 24 h at 4°C then further stained with an anti-lucifer yellow antibody (1 : 50,000, Molecular Probes) for 5 days at 4°C and visualized with Cy3-conjugated Donkey anti-rabbit IgG (1 : 400, Jackson ImmunoResearch) for 3 h at 4°C.

**Quantitative morphological analyses of dendritic spines.** All images were processed using the Image J software program (National Institutes of Health, Bethesda, MD, USA). Images were obtained with 100 × 1.4 NA oil-immersion lenses using the C2si Confocal Laser Microscope (Nikon). Stacks of 70–90 serial optical sections were obtained from each cerebral cortex (22–27 dendrites from 10–15 cells from three animals). The spine density was determined by manually identifying the spines and using 3D images to measure the dendrite length with the Simple Neurite Tracer plug-in<sup>40</sup>.

**Electrophysiological recordings.** Transverse slices (200 μm thick) were cut from the cerebral cortex using a vibratome. The slice patch analyses were performed according to a similar previously reported method<sup>41</sup>. ACSF contained (in mM): 117 NaCl, 3.6 KCl, 2.5 CaCl<sub>2</sub>, 1.2 MgCl<sub>2</sub>, 1.2 NaH<sub>2</sub>PO<sub>4</sub>, 25 NaHCO<sub>3</sub> and 11 glucose saturated with 95% O<sub>2</sub> and 5% CO<sub>2</sub>. The recordings were made from pyramidal neurons in layer 2/3 of the primary cerebral cortex (10–20 cells from 3–4 slices from 3 animals). Patch pipettes (5–10 MΩ) were filled with an internal solution containing the following components (in mM): 135 potassium gluconate, 5 KCl, 0.5 CaCl<sub>2</sub>, 2 MgCl<sub>2</sub>, 5 EGTA, 5 HEPES and 5 ATP-Mg. All recordings were made at a holding potential of -70 mV. mEPSCs were recorded in the presence of 1 μM TTX and 10 μM bicuculline methiodide, a competitive GABA<sub>A</sub> receptor antagonist. The data were stored according to a previous report<sup>41</sup>. In some experiments, the cortical slices were incubated with ACSF, 50 nM hrCatS (R&D Systems), heat-denatured hrCatS or 50 nM hrCatS in combination with 20 μM Z-FL-COCHO for 3 h before patch clamp recordings were obtained from the cortical neurons.

**Two-photon microscopy.** Under ketamine and xylazine (100 mg kg<sup>-1</sup> and 10 mg kg<sup>-1</sup>) anesthesia, a custom-made metal plate was fixed to the skull and attached to a stereotaxic apparatus. Then a craniotomy (3 mm in diameter) was performed in the cerebral cortex, and the dura was carefully removed. Images were obtained with an Olympus 25 × 1.0 NA water-immersion lens and a Spectra Physics Mai-Tai IR laser tuned at 890 nm for two-photon excitation of GFP ( $n = 3$  animals). A glass capillary (tip diameter 3 ~ 6 μm) filled with ATP (1 mM) and 0.5% rhodamine-dextran in ACSF was inserted into the brain (50–100 μm in depth) and z-stacked images were obtained from 15 μm above to 15 μm underneath the tip of the capillary. AR-C 66096 (a P2Y<sub>12</sub>R inhibitor, 10 μM; Tocris) and Z-FL-COCHO (a CatS inhibitor, 1 μM; Merck) in ACSF was applied on the brain, the same as for the lens immersion ACSF. Then after 15 min of incubation, the imaging was restarted at a site at least 400 μm from the site of the first ATP trial. The total pixels in the area were analyzed.

**Statistical analyses.** All data are shown as the mean ± SEM. The statistical analyses were performed using two-tailed unpaired Student's *t*-test, a one-way analysis of variance (ANOVA) with a post hoc Tukey's test or a two-way ANOVA with repeated measurements using the GraphPad Prism Software package (GraphPad Software Inc., San Diego, CA, USA). Unless otherwise indicated, the data met the assumptions of equal variances. Differences were considered to be significant at  $P < 0.05$ .



1. Tremblay, M. E. *et al.* The role of microglia in the healthy brain. *J. Neurosci.* **31**, 16064–16069 (2011).
2. Davalos, D. *et al.* ATP mediates rapid microglial response to local brain injury in vivo. *Nat. Neurosci.* **8**, 752–758 (2005).
3. Nimmerjahn, A., Kirchhoff, F. & Helmchen, F. Resting microglial cells are highly dynamic surveillants of brain parenchyma in vivo. *Science* **308**, 1314–1318 (2005).
4. Wake, H., Moorhouse, A. J., Jinno, S., Kohsaka, S. & Nabekura, J. Resting microglia directly monitor the functional state of synapses in vivo and determine the fate of ischemic terminals. *J. Neurosci.* **29**, 3974–3980 (2009).
5. Schafer, D. *et al.* Microglia sculpt postnatal neural circuits in an activity and complement-dependent manner. *Neuron* **74**, 691–705 (2012).
6. Paolicelli, R. C. *et al.* Synaptic pruning by microglia is necessary for normal brain development. *Science* **333**, 1456–1458 (2011).
7. Roumier, A. *et al.* Impaired synaptic function in the microglial KARAP/DAP12-deficient mouse. *J. Neurosci.* **24**, 11421–11428 (2004).
8. Hoshiko, M., Arnoux, I., Avignone, E., Yamamoto, N. & Audinat, E. Deficiency of the microglial receptor CX3CR1 impairs postnatal functional development of thalamocortical synapses in the barrel cortex. *J. Neurosci.* **32**, 15106–15111 (2012).
9. Derecki, N. *et al.* Wild-type microglia arrest pathology in a mouse model of Rett syndrome. *Nature* **484**, 105–109 (2012).
10. Chen, S. *et al.* Hematopoietic origin of pathological grooming in Hoxb8 mutant mice. *Cell* **141**, 775–785 (2010).
11. Petanceska, S., Canoll, P. & Devi, L. A. Expression of rat cathepsin S in phagocytic cells. *J. Biol. Chem.* **271**, 4403–4409 (1996).
12. Sukhova, G. K. *et al.* Deficiency of cathepsin S reduces atherosclerosis in LDL receptor-deficient mice. *J. Clin. Invest.* **111**, 897–906 (2003).
13. Nishioku, T. *et al.* Involvement of cathepsin E in exogenous antigen processing in primary cultured murine microglia. *J. Biol. Chem.* **277**, 4816–4822 (2002).
14. Nakagawa, T. Y. *et al.* Impaired invariant chain degradation and antigen presentation and diminished collagen-induced arthritis in cathepsin S null mice. *Immunity* **10**, 207–217 (1999).
15. Clark, A. K. *et al.* Inhibition of spinal microglial cathepsin S for the reversal of neuropathic pain. *Proc. Natl. Acad. Sci. U. S. A.* **104**, 10655–10660 (2007).
16. Liu, Z. W., Faraguna, U., Cirelli, C., Ttononi, G. & Gao, X. B. Direct evidence for wake-related increases and sleep-related decreases in synaptic strength in rodent cortex. *J. Neurosci.* **30**, 8671–8675 (2010).
17. Vyazovskiy, V. V., Cirelli, C., Pfister-Genskow, M., Faraguna, U. & Ttononi, G. Molecular and electrophysiological evidence for net synaptic potentiation in wake and depression in sleep. *Nat. Neurosci.* **11**, 200–208 (2008).
18. Maret, S., Faraguna, U., Nelson, A. B., Cirelli, C. & Ttononi, G. Sleep and waking modulate spine turnover in the adolescent mouse cortex. *Nat. Neurosci.* **14**, 1418–1420 (2011).
19. Yang, G. & Gan, W. B. Sleep contributes to dendritic spine formation and elimination in the developing mouse somatosensory cortex. *Developmental neurobiology* **72**, 1391–1398 (2012).
20. Gekakis, N. *et al.* Role of the CLOCK protein in the mammalian circadian mechanism. *Science* **280**, 1564–1569 (1998).
21. Nakanishi, H. Microglial functions and proteases. *Mol. Neurobiol.* **27**, 163–176 (2003).
22. Wang, D. & Fawcett, J. The perineuronal net and the control of CNS plasticity. *Cell Tissue Res.* **349**, 147–160 (2012).
23. Nakanishi, H. *Proteases and Synaptic Activity*. vol. 3. Springer Netherlands, (2005).
24. Sangoram, A. M. *et al.* Mammalian circadian autoregulatory loop: a timeless ortholog and mPer1 interact and negatively regulate CLOCK-BMAL1-induced transcription. *Neuron* **21**, 1101–1113 (1998).
25. Kume, K. *et al.* mCRY1 and mCRY2 are essential components of the negative limb of the circadian clock feedback loop. *Cell* **98**, 193–205 (1999).
26. Haynes, S. E. *et al.* The P2Y12 receptor regulates microglial activation by extracellular nucleotides. *Nat. Neurosci.* **9**, 1512–1519 (2006).
27. McClung, C. A. *et al.* Regulation of dopaminergic transmission and cocaine reward by the Clock gene. *Proc. Natl. Acad. Sci. U. S. A.* **102**, 9377–9381 (2005).
28. Roybal, K. *et al.* Mania-like behavior induced by disruption of CLOCK. *Proc. Natl. Acad. Sci. U. S. A.* **104**, 6406–6411 (2007).
29. Mataga, N., Mizuguchi, Y. & Hensch, T. K. Experience-dependent pruning of dendritic spines in visual cortex by tissue plasminogen activator. *Neuron* **44**, 1031–1041 (2004).
30. Liuzzo, J. P., Petanceska, S. S., Moscatelli, D. & Devi, L. A. Inflammatory mediators regulate cathepsin S in macrophages and microglia: A role in attenuating heparan sulfate interactions. *Mol. Med.* **5**, 320–333 (1999).
31. Bromme, D. *et al.* Functional expression of human cathepsin S in *Saccharomyces cerevisiae*. Purification and characterization of the recombinant enzyme. *J. Biol. Chem.* **268**, 4832–4838 (1993).
32. Hering, H. & Sheng, M. Dendritic spines: structure, dynamics and regulation. *Nat. Rev. Neurosci.* **2**, 880–888 (2001).
33. Berardi, N., Pizzorusso, T. & Maffei, L. Extracellular matrix and visual cortical plasticity: freeing the synapse. *Neuron* **44**, 905–908 (2004).
34. Ethell, I. M. & Yamaguchi, Y. Cell surface heparan sulfate proteoglycan syndecan-2 induces the maturation of dendritic spines in rat hippocampal neurons. *J. Cell Biol.* **144**, 575–586 (1999).
35. Ethell, I. M. *et al.* EphB/syndecan-2 signaling in dendritic spine morphogenesis. *Neuron* **31**, 1001–1013 (2001).
36. Irie, F., Badie-Mahdavi, H. & Yamaguchi, Y. Autism-like socio-communicative deficits and stereotypies in mice lacking heparan sulfate. *Proc. Natl. Acad. Sci. U. S. A.* **109**, 5052–5056 (2012).
37. Koyanagi, S. *et al.* cAMP-response element (CRE)-mediated transcription by activating transcription factor-4 (ATF4) is essential for circadian expression of the Period2 gene. *J. Biol. Chem.* **286**, 32416–32423 (2011).
38. Cavadini, G. *et al.* TNF-alpha suppresses the expression of clock genes by interfering with E-box-mediated transcription. *Proc. Natl. Acad. Sci. U. S. A.* **104**, 12843–12848 (2007).
39. Elston, G. N., Oga, T. & Fujita, I. Spinogenesis and pruning scales across functional hierarchies. *J. Neurosci.* **29**, 3271–3275 (2009).
40. Cardona, A. *et al.* Identifying neuronal lineages of *Drosophila* by sequence analysis of axon tracts. *J. Neurosci.* **30**, 7538–7553 (2010).
41. Yamada, J. *et al.* Reduced synaptic activity precedes synaptic stripping in vagal motoneurons after axotomy. *Glia* **56**, 1448–1462 (2008).

## Acknowledgements

This work was supported by the Core Research for Evolutional Science and Technology (CREST) program of the Japan Science and Technology (JST) Corporation.

## Author contributions

Y.H. and H.N. designed the experiments. Y.H. performed the experiments and analyzed the immunohistochemical, electrophysiological and EEG data. S.K. and N.K. performed the experiments and analyzed the expression of the clock genes. S.K. and N.K. also constructed the luciferase reporter assay system. R.O. and Z.W. performed the isolation of microglia from the adult brains. K.U. provided technical support for the measurement of the EEG and the spontaneous locomotor activity. H.T.-S. performed the *in vivo* imaging. S.K. generated the Iba-EFPFP mice. Y.H., S.K., N.K., R.O., Z.W., H.T.-S., S.J., K.L., S.O. and H.N. analyzed the data and interpreted the results. All authors discussed and agreed on the results and commented on the manuscript. Y.H. and H.N. wrote the manuscript. H.N. supervised the work.

## Additional information

**Supplementary information** accompanies this paper at <http://www.nature.com/scientificreports>

**Competing financial interests:** The authors declare no competing financial interests.

**How to cite this article:** Hayashi, Y. *et al.* The intrinsic microglial molecular clock controls synaptic strength via the circadian expression of cathepsin S. *Sci. Rep.* **3**, 2744; DOI:10.1038/srep02744 (2013).



This work is licensed under a Creative Commons Attribution-NonCommercial-ShareAlike 3.0 Unported license. To view a copy of this license, visit <http://creativecommons.org/licenses/by-nc-sa/3.0>